Magnetic behaviour and magnetostriction of $Tb_xY_{1-x}Mn_2$ intermetallics

Magnetic behaviour and magnetostriction of $Tb_x Y_{1-x} Mn_2$ intermetallics

J M de Teresa†, M R Ibarra†, C Ritter†‡, C Marquina†, Z Arnold†§ and A del Moral†

† Departamento de Física de la Materia Condensada e Instituto de Ciencia de Materiales de Aragón, Universidad de Zaragoza–CSIC, 50009 Zaragoza, Spain
‡ Institut Laue–Langevin, Grenoble Cédex, France
§ Institute of Physics, Czech Academy of Sciences, Cukrovarnicka 10, 162 00 Praha 6, Czech Republic

Abstract. The spontaneous magnetic behaviour and the stability of the magnetic moment on the Mn atoms versus temperature, with concentration, and under applied magnetic field and pressure in the series $Tb_x Y_{1-x} Mn_2$ have been investigated by means of magnetostriction up to 14 T, AC susceptibility under pressure up to 7 kbar and linear thermal expansion measurements. Large volume anomalies were observed in all compounds of the series at T_N, the temperature at which the Mn magnetic moments become local. T_N remains almost constant for $x \geqslant 0.2$. Below T_N the magnetic structure of Tb-rich compounds is unstable under applied magnetic field and the Mn magnetic moments can be reverted to itinerancy. The obtained results can be explained on the assumption that the transition is non-homogeneous and consequently a small part of the sample does not transform, remaining without Mn local magnetic moments below T_N. This region grows either under applied field or under applied pressure and it can occupy the whole sample. From these results a magnetic phase diagram of this series is proposed.

1. Introduction

Research on RMn_2 compounds (where R = rare earth) has been widely developed in recent years due to the behaviour of the magnetic moment at the manganese sites (μ_{Mn}). The RMn_2 compounds crystallize in the Laves phases structures. The hexagonal C14 phase is found for R = Lu, Pr, Nd, Sm, Ho, Er, Tm and Th and the cubic C15 phase for R = Y, Gd, Tb, Dy and Ho. It is well known that for R = Tb, Gd, Sm, Nd, Pr and Y, μ_{Mn} is intrinsic below T_N [1] and for R = Dy and Ho it is induced by the strong molecular field from the rare earth sites [2, 3].

The existence of a Mn–Mn critical distance (≈ 2.676 Å) has often been assumed to account for the experimental facts. However theoretical studies on the RMn_2 band structure [4–6] and recent x-ray absorption experiments using synchrotron radiation [7] seem to question such a naïve picture.

The appearance of a magnetic moment on Mn takes place through a temperature-induced first-order transition. This transition (at around 100 K or less) brings about very large magnetovolume effects. Thermal expansion and magnetostriction measurements are powerful tools to detect the transition [8, 9].

At the transition temperature (T_N), a very large spontaneous expansion (5% in YMn_2, 1.5% in $TbMn_2$) is observed along with a paramagnetic–antiferromagnetic transition. This

high-volume phase is unstable under applied magnetic field in $TbMn_2$ but stable in YMn_2 up to 14 T [8]. Magnetostriction and thermal expansion under steady magnetic fields measurements confirmed these facts [9–11]. YMn_2 and $TbMn_2$ compounds have been thoroughly studied in the last years. Neutron diffraction [12–14], magnetization [15], thermal expansion [10], magnetostriction [10] and low-field AC susceptibility [16] experiments on $TbMn_2$ were interpreted as follows [16]: at $T_N \approx 45$ K, part of the sample, the transformed phase (TP), suffers a paramagnetic–antiferromagnetic transition giving rise to the S_1 magnetic structure [12], where the Mn atoms carry a $2.5\mu_B$ magnetic moment. This transition is responsible for the large magnetovolume effects observed below T_N. At around the same temperature, the rest of the sample, the non-transformed phase (NTP), undergoes a paramagnetic–ferrimagnetic transition, with no magnetic moment at the Mn sites. At $T_c \approx 35$ K there is a magnetic transition in the NTP phase to the $S2$ structure, which is reminiscent of the $DyMn_2$-like magnetic structure [2], where a small magnetic moment is induced on Mn. Under applied field or pressure, the NTP phase grows whereas the TP phase is reduced. At $H \approx 7$ T or $P \approx 2$ kbar the whole sample is found in the NTP phase.

In YMn_2 a first-order paramagnetic–antiferromagnetic transition is observed at $T_N \approx 70$–100 K. The $2.8\mu_B$ Mn magnetic moments set in an antiferromagnetic helix through the whole sample at ambient pressure [17, 18]. The external pressure on the sample reduces the Néel temperature and the thermal expansion jump at T_N [14, 19]. As the pressure is increased the NTP phase grows. At $P \approx 2.7$ kbar there is no longer evidence of either lattice expansion or long-range magnetic order. The YMn_2 antiferromagnetic structure and the intrinsic μ_{Mn} are stable under applied magnetic field [9].

Our work on $Tb_x Y_{1-x} Mn_2$ is intended to find out how the Néel temperature, T_N (≈ 100 K in YMn_2 and ≈ 45 K in $TbMn_2$) and the magnetic behaviour change through the series under different external conditions. The $TbMn_2$ low-temperature magnetic structure is very different from the YMn_2 one. As the yttrium content is increased a continuous change from one structure to the other can occur even though a sudden change to a new magnetic structure at an intermediate yttrium composition is also possible as it happens in $Dy_x Y_{1-x} Mn_2$, [20] which richness of phenomena has encouraged us to carry out this work.

As far as we know scarce information has been reported on this series. Magnetization and powder neutron diffraction studies [21] seem to indicate that in the yttrium-rich compounds the magnetic structure keeps the YMn_2-like structure. In the terbium-rich compounds the neutron diffraction data below T_N show a structure reminiscent of the S_1-type structure found in $TbMn_2$. In the intermediate concentration range coexistence of the $TbMn_2$-like and YMn_2-like magnetic structures seems to be present. Pioneer studies on the magnetic properties of the system $Tb_x Y_{1-x} Mn_2$ [22, 23] led to a set of conclusions that should come under review in the light of the new models on RMn_2 and also due to the significant discrepancies between such previous measurements and our experimental results. We have performed linear thermal expansion (LTE) measurements in order to detect T_N (the onset of magnetic moment at the Mn sites) and the magnitude of the spontaneous magnetovolume effect that this transition brings about. Magnetostriction (MS) measurements under applied magnetic fields up to 14 T were performed in order to probe the stability of the low-temperature magnetic structures. Low-field AC susceptibility (χ_{AC}) measurements allowed us to detect magnetic transitions in the NTP phase. The study of the magnetic behaviour under pressure in each compound of the series provides relevant information on the ground state of the system as a function of temperature under zero pressure.

2. Experiments

The polycrystalline compounds $Tb_xY_{1-x}Mn_2$ (with $x = 0.2$, 0.4, 0.6, 0.8) were prepared by arc melting the high-purity constituents, R (99.9%) and Mn (99.99%). 3% of rare earth element was added over the nominal concentration in order to avoid the formation of the secondary phase R_6Mn_{23}. The samples were melted several times and subsequently annealed for five days at 800 °C under a stabilized argon atmosphere. The presence of the C15 cubic Laves phase and the absence of any secondary phases was confirmed by x-ray powder diffraction.

LTE and MS measurements were performed using the strain gauge technique and a modified Wheastone bridge. One of the arms is the active gauge (Micromeasurements SK-350) glued on the sample and other one is a dummy gauge, cemented on a silica disc, in order to compensate spurious thermal or magnetoresistance effects. The volume thermal expansion is straightforwardly calculated as three times the LTE, $\omega = \Delta V/V = 3 \Delta L/L$, as long as the polycrystalline sample is homogeneous. By means of the strain gauge technique, the magnetostriction parallel, $\lambda_{\parallel}$, and perpendicular, $\lambda_{\perp}$, to the applied magnetic field can be measured in polycrystalline samples. From $\lambda_{\parallel}$ and $\lambda_{\perp}$, the anisotropic, λ_t, and volume, ω, magnetostrictions are obtained as $\lambda_t = \lambda_{\parallel} - \lambda_{\perp}$ and $\omega = \lambda_{\parallel} + 2\lambda_{\perp}$ respectively. In the pulsed magnetic field installation, an AC bridge working with a carrier frequency of 25 kHz is used. The high pulsed magnetic field of peak value 14.2 T and 50 ms pulse width was produced by discharging a capacitor bank on a copper wire wound coil immersed in liquid nitrogen. The strain $\Delta L/L$ is measured in both techniques within an accuracy of 10^{-6}. The low-field AC susceptibility, χ_{AC} (T), was measured using a low-frequency (15 Hz) mutual inductance bridge, with a peak value of the magnetic field of $\approx$30 mOe. The high-pressuse measurements were done using a CuBe cell under fixed hydrostatic pressures up to 10 kbar. The pressure was measured *in situ*, using a manganin pressure sensor. All the measurements were performed in the temperature range between 4.2 and 300 K by using a liquid helium continuous-flow cryostat.

3. Results and discussion

3.1. Thermal expansion

The LTEs of the four $Tb_xY_{1-x}Mn_2$ samples ($x = 0.2$, 0.4, 0.6, 0.8) were firstly measured by cooling down from room temperature to 4 K and subsequently by heating up to room temperature. In figure 1 we show the results of the heating process of the x= 0.4, 0.6 and 0.8 samples and the cooling process of the $x = 0.2$ sample. All the compounds undergo an abrupt volume change at around 40 K marking the change from itinerant to local magnetism. The appearance of a local magnetic moment at the manganese sites is responsible for this behaviour. In the $x = 0.2$ compound the jump is smaller in the heating process than in the cooling process. This fact is related to the sample cracks which appear in the cooling process passing through the Néel temperature. Due to the huge volume expansion involved ($\approx$2.5%) the sample breaks in the cooling process and the drop that is observed in the heating process does not match the jump in the cooling process. This feature is observed in YMn_2 as well. Therefore we show the cooling process of $Tb_{0.2}Y_{0.8}Mn_2$ because it is more reliable. The LTE coefficient $\alpha = (1/L)(\partial L/\partial T)$ displays a large value at room temperature in the four samples ($\approx$35 $\times$ 10^{-6} K^{-1}, to be compared with $\alpha \approx 15 \times 10^{-6}$ K^{-1} in a normal metal). This is a hallmark of the existence of spin fluctuations according to Moriya's theory [24]. The temperature T_N, at which local magnetic moments appear at the Mn sites in the
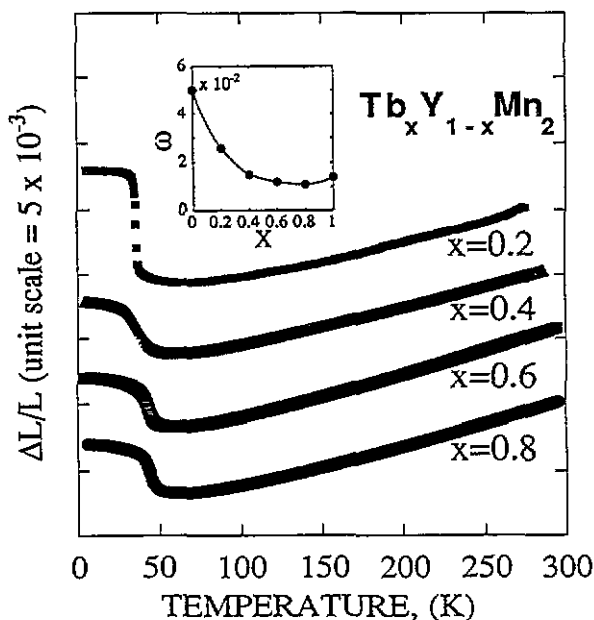
Figure 1. Linear thermal expansion of $Tb_xY_{1-x}Mn_2$ ($x = 0.8$, 0.6, 0.4 and 0.2) compounds as a function of temperature. The inset shows the volume anomaly at T_N as a function of x. The line is a visual guide.

TP phase, unexpectedly remains independent of the yttrium concentration across the entire concentration range $1 \geqslant x \geqslant 0.2$ even though $TbMn_2$ and YMn_2 have different T_N: 45 K and 100 K respectively. T_N is calculated with the help of the LTE coefficient, which shows a sharp peak at the transition temperature ($T_N = 43.5$, 42.7, 35 and 48.5 K in the $x = 0.8$, 0.6, 0.4 and 0.2 compounds respectively in the heating process). Therefore T_N is around 45 K in the concentration range $0.2 \leqslant x \leqslant 1$. The inset of figure 1 shows the spontaneous volume change passing through T_N for the whole series (the $TbMn_2$ and YMn_2 data are obtained from [1]). This change ($\approx 1.5\%$) remains almost constant in the concentration range $0.4 \leqslant x \leqslant 1$ and grows when x approaches the value $x = 0$ ($\approx 5\%$). These values fully agree with the neutron diffraction estimate [21] but disagree with the thermal expansion measurements reported elsewhere [22]. The magnetic structure, evolving from the $TbMn_2$ structure to the YMn_2 structure, is thought to be responsible for the increasing magnitude of the jump.

3.2. Volume magnetostriction

The volume magnetostriction of $TbMn_2$ and YMn_2 has been reported elsewhere [8–10]. The volume magnetostriction (up to 12 T) of YMn_2 was found to be negligible and consequently the magnetic structure of YMn_2 was considered to be stable under applied magnetic field [9]. Nevertheless the magnetic structure of $TbMn_2$ in the TP phase (S_1 type [12]) is unstable under applied magnetic field and a large volume magnetostriction ($\omega \approx 1.7 \times 10^{-2}$) can be observed below T_N. This is associated with the field-induced transition to the NTP phase, which is the low-volume phase [10]. In figure 2 we show the volume magnetostriction isotherms of the $x = 0.8$, 0.6 and 0.4 compounds. The magnetostrictive effects on $Tb_{0.2}Y_{0.8}Mn_2$ are very small and are not shown here. The volume
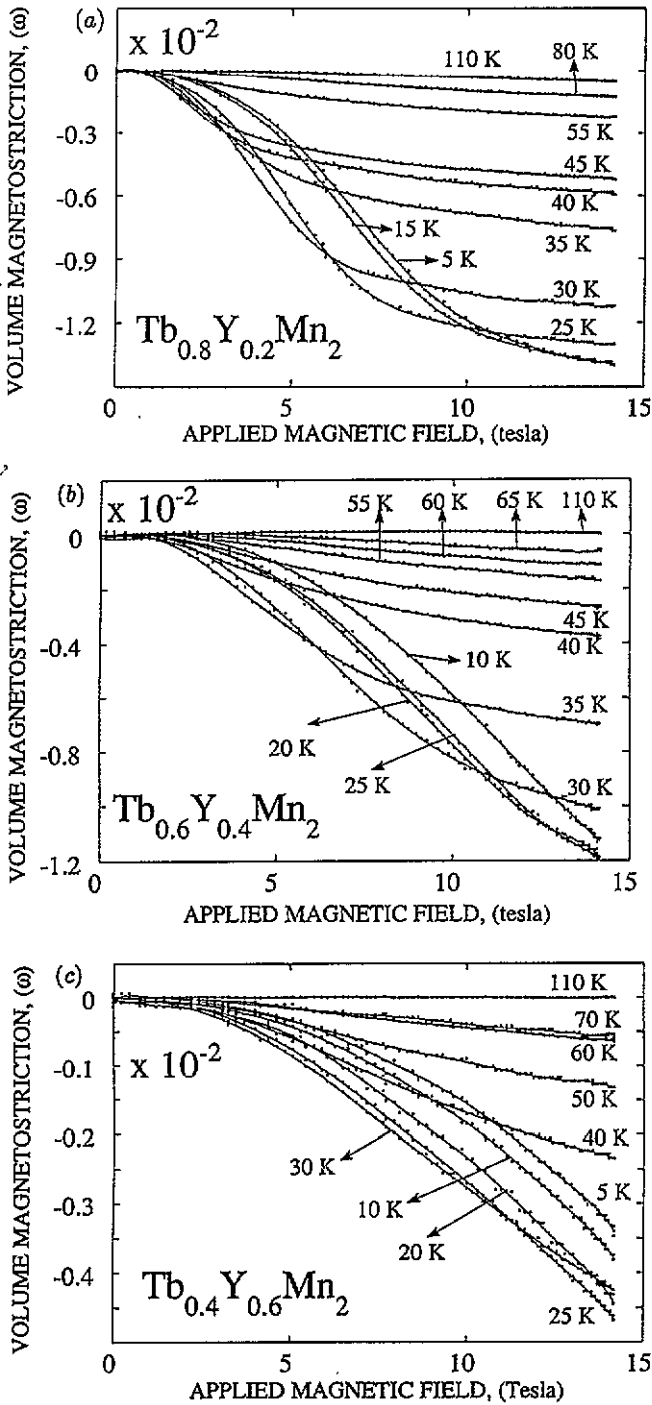
Figure 2. Isotherms of the forced volume magnetostriction, ω, for $Tb_x Y_{1-x} Mn_2$ with $x = 0.8$ (a), $x = 0.6$ (b) and $x = 0.4$ (c). Lines are visual guides.

magnetostriction isotherms are useful to determine the critical field at each temperature (this field is defined as the minimum magnetic field necessary to suppress the Mn local magnetic moment and revert the whole sample to the low-volume (NTP) phase [10]; the critical field (H_c) is attained when the isotherms begin to saturate). For all the compositions the volume magnetostriction is small (and with a field quadratic dependence) above T_N as is to be expected in the paramagnetic regime [27]. At around 45 K the shape of the isotherms begins to change. In $Tb_{0.8}Mn_{0.2}Mn_2$ (figure 2(a)) two regimes are clearly seen below T_N. At low fields there is a rapid increase of the striction and then a tendency to saturation is observed at greater fields. The same behaviour is found for $Tb_{0.6}Y_{0.4}Mn_2$ (figure 2(b)) although the tendency to saturation is not apparent below 30 K. The large volume magnetostriction below T_N is associated with the instability of the μ_{Mn} under applied magnetic field. The magnetic field reverts the manganese moments to itineracy and the low-volume (NTP) phase is recovered. In $Tb_{0.4}Y_{0.6}Mn_2$ (figure 2(c)) the maximum available field (14 T) is not strong enough to revert the whole sample to the NTP phase below 40 K. Regarding the critical field, H_c, there are two remarkable features. Firstly, in all the compounds, as the temperature goes down the critical field becomes higher. In the $x = 0.8$ compound, H_c is around 5 T at 35 K, 8 T at 25 K and 13 T at 15 K. This means that the high-volume magnetic structure (TP phase) is stabilized by lowering the temperature. The same trend was found in $TbMn_2$ [10]. The second remarkable feature is that the critical field at a fixed temperature is greater as the yttrium content increases. In fact, in the $x = 0.6$ sample, H_c is around 10 T at 35 K and greater than the maximum attainable field (14 T) at temperatures lower than 30 K. In the $x = 0.4$ compound, H_c is greater than 14 T at temperatures lower than 40 K. In figure 3 we show the temperature dependence of the volume magnetostriction at the maximum available field. Above T_N the ω values are very small for all the compounds. When passing through T_N a rapid increase is observed. In the $x = 0.8$ and 0.6 compounds the volume magnetostriction below T_N reaches values of $\omega \approx -1.4 \times 10^{-2}$ and $\omega \approx -1.2 \times 10^{-2}$ respectively, which approximately equal the *spontaneous* volume strictions measured by LTE (see figure 1). However in the $x = 0.4$ compound the volume magnetostriction only reaches one-third of the volume striction measured by LTE. We can infer from the volume magnetostriction results that the magnetic structures of the $x = 0.8$ and 0.6 compounds must be very close to the $TbMn_2$-like magnetic structure. Consequently the magnetic field is able to suppress the local magnetic moment at the manganese sites and revert the whole sample to the NTP phase, where the Tb magnetic moments govern the magnetism. In the $x = 0.4$ compound the available magnetic field is lower than H_c. As a consequence we can assume that only a part of the TP phase is reverted to the NTP phase at 14 T. These results suggest that the zero-field structure is not exactly the $TbMn_2$-like one. One possibility is the appearance of a new ground state in this intermediate range of concentration characterized by the existence of short-range order as was found in the (Dy–Y)Mn$_2$ series. A further study of the changes in these magnetic structures under pressure using neutron diffraction experiments would clear up this point. In the $Tb_{0.2}Y_{0.8}Mn_2$ compound the negligible volume magnetostriction above and below T_N leads to the assumption of a YMn_2-like magnetic structure. In figure 3 it is also remarkable that for the $x = 0.6$ and $x = 0.4$ compounds the volume magnetostriction diminishes below 20 K instead of remaining constant. That is so because the critical field is greater as the temperature is lowered. It indicates that the TP phase gains stability when the temperature is lowered and a field greater than 14 T is needed to revert the whole sample to the NTP phase. In the $x = 0.8$ compound H_c is less than 14 T at all temperatures and the whole sample is reverted to the NTP phase. The volume magnetostriction at 14 T consequently remains constant down to 4 K.
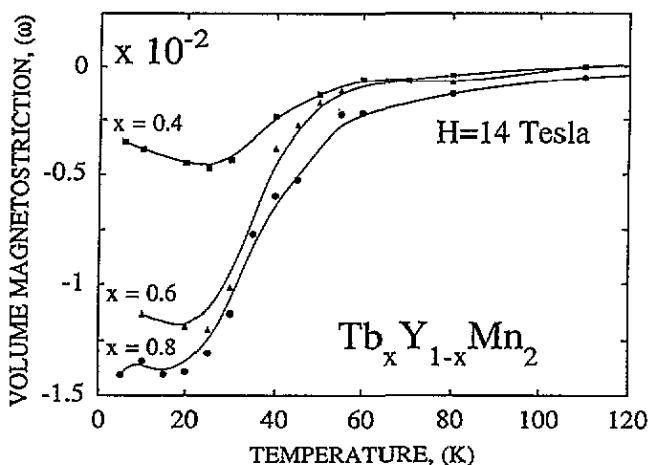
Figure 3. Volume magnetostriction at 14 T of $Tb_xY_{1-x}Mn_2$ with $x = 0.8$, 0.6 and 0.4 as a function of temperature. Lines are visual guides.

3.3. Anisotropic magnetostriction

In figure 4 we show the λ_t isotherms above and below T_N for all compositions. In the $x = 0.8$ and $x = 0.6$ compounds the field dependence of λ_t below T_N can be explained as follows: at low fields a rapid increase of λ_t is thought to appear due to the field-induced change from the TP phase to the NTP phase. The TP phase is antiferromagnetic and therefore its contribution to the λ_t is negligible. For that reason the NTP phase is the source of the measured λ_t. As in $TbMn_2$, a rhombohedral distortion [25] is expected if the Tb^{3+} magnetic moments lie along the [111] easy magnetization direction (EMD) in the NTP phase. When the applied field attains the critical field, the NTP phase spreads throughout the sample and for fields greater than the critical field a tendency to saturation is observed. The explanation of the low-temperature behaviour of $Tb_{0.4}Y_{0.6}Mn_2$ is similar but, as the critical field is greater than the maximum applied field, the NTP phase is not completely developed. The temperature dependence of the critical field follows the same trend observed through the volume magnetostriction isotherms. The value of the λ_t at fixed field and temperature is lower as the yttrium content increases. Two facts are responsible for this behaviour: there are fewer Tb^{3+} magnetic moments contributing to λ_t within the NTP phase in the yttrium-rich compounds and a smaller part of the TP phase is transformed into the NTP phase. Above T_N the isotherms display the typical behaviour of an approaching paramagnetic–ferromagnetic phase transition (with a quadratic field dependence well above T_N).

3.4. Susceptibility measurements under hydrostatic pressure

The low-field AC magnetic susceptibility measurements turned out to be very useful in order to detect transitions in several RMn_2 compounds [2, 16]. This fact encouraged us to carry out χ_{AC} measurements on $Tb_xY_{1-x}Mn_2$ under pressures ranging from 0 kbar to 7 kbar. In figure 5 we show the results for the $x = 1$, 0.8 and 0.6 compounds. The instability of the TP phase of $TbMn_2$ and YMn_2 under pressures higher than 3 kbar has been proved extensively [14, 16, 19, 26]. Therefore the suppression of the TP phase is expected in all $Tb_xY_{1-x}Mn_2$ compounds under high enough applied pressures and thus the whole sample
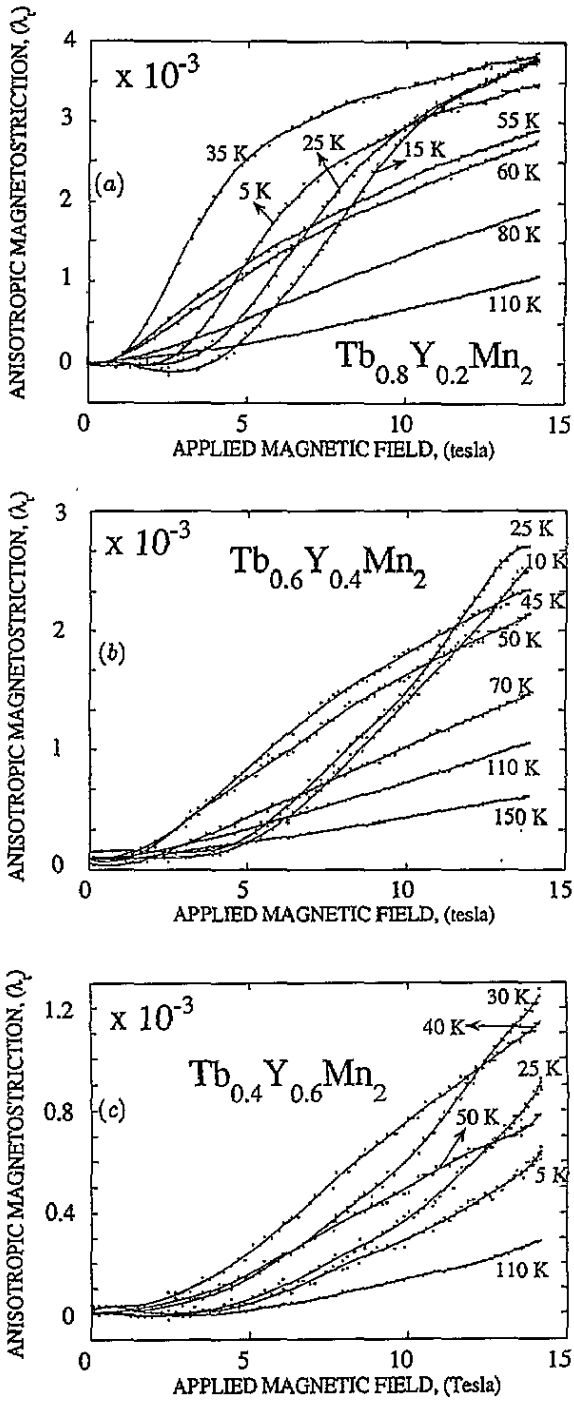
Figure 4. Isotherms of the forced anisotropic magnetostriction, λ_t, for $Tb_xY_{1-x}Mn_2$ with $x = 0.8$ (a), $x = 0.6$ (b) and $x = 0.4$ (c). Lines are visual guides.
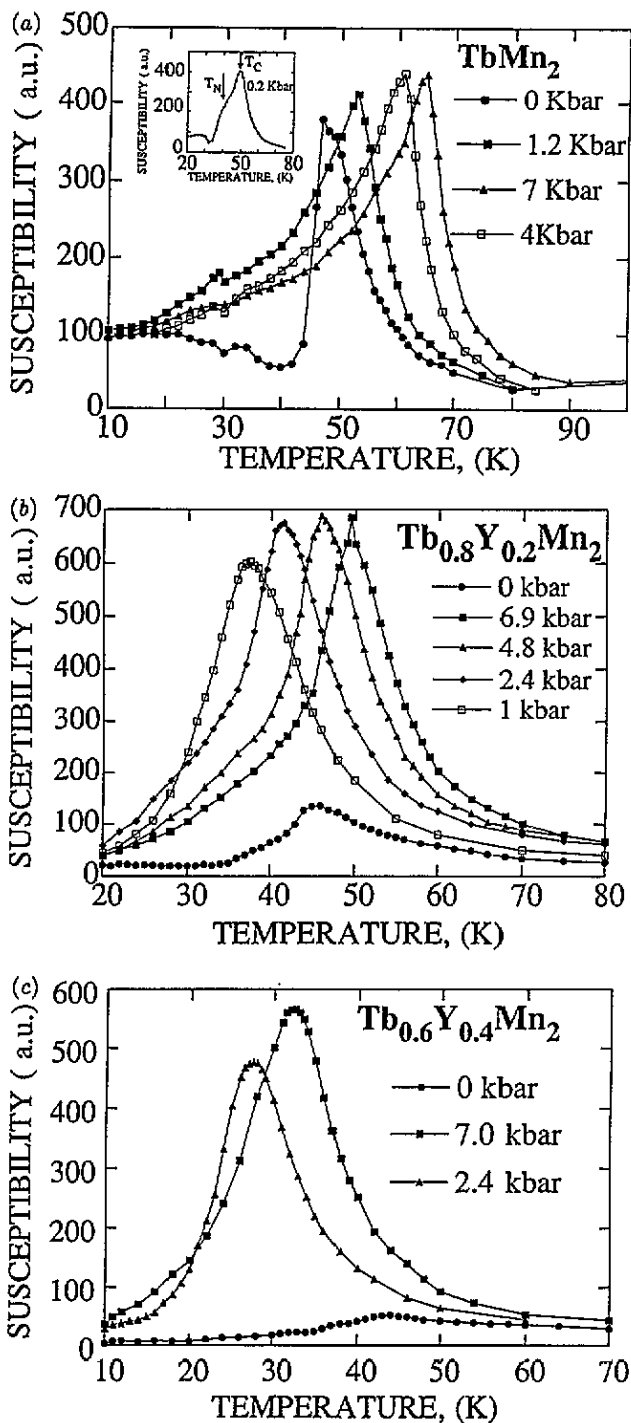
Figure 5. AC susceptibility of $Tb_x Y_{1-x} Mn_2$ with $x = 1$ (a) (the inset shows the $p = 0.2$ kbar measurement for the sake of clarity), $x = 0.8$ (b) and $x = 0.6$ (c) as a function of temperature under different pressures. Lines are visual guides.
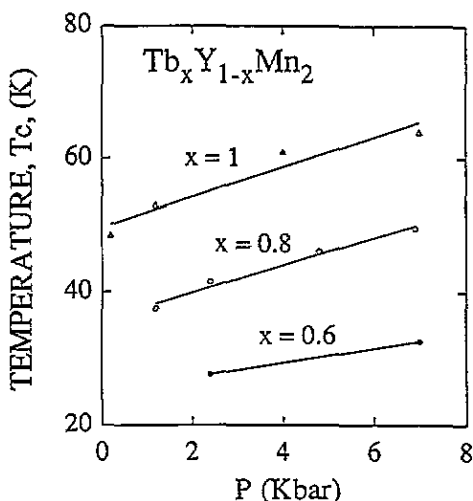
Figure 6. Pressure dependence of T_c, the transition temperature in the NTP phase of $Tb_x Y_{1-x} Mn_2$ ($x = 1$, 0.8, 0.6) compounds. Lines are linear fits.

would remain as NTP phase and would order at T_c, which is the ordering temperature within the NTP phase. In $TbMn_2$ (figure 5(a)) a hump can be observed at T_N and a peak appears at T_c under 0.2 kbar applied pressure (inset of figure 5(a)). At ambient pressure T_N and T_c merge and the T_c sharp peak masks the T_N hump. Under 1.2 kbar and greater pressures most of the sample remains as NTP phase and only T_c becomes visible. Neutron diffraction measurements under pressure confirmed that the TP phase must have disappeared completely under 2 kbar in $TbMn_2$ and 2.7 kbar in YMn_2 [14]. In figure 5(b) and 5(c) we show the χ_{AC} measurements of the $x = 0.8$ and 0.6 compounds. For these compounds T_c should be below T_N under ambient pressure because the terbium content is lower than in $TbMn_2$, where $T_N = T_c$ However it is very difficult to obtain T_c directly from the low-pressure measurements because at T_c the sample is supposed to be mainly (or completely) TP phase. We think that the humps which are observed at ambient pressure in the $x = 0.8$ and $x = 0.6$ compounds should be attributed to T_N. As the pressure is increased, the TP phase becomes unstable and the peak associated with the para–ferromagnetic transition within the NTP phase becomes visible. Above a critical pressure the TP phase is thought to disappear completely as occurs in $TbMn_2$ and YMn_2 [14, 16]. In figure 6 we show the dependence of T_c on pressure according to χ_{AC} high-pressure measurements in the $x = 1, 0.8$ and 0.6 compounds. The linear behaviour of T_c with pressure (up to 8 kbar) has also been observed in resistivity measurements of several RMn_2 compounds [28]. A neutron diffraction experiment under pressure is in progress to find out the percentages of the sample which are in the TP and NTP phases respectively under each pressure below the critical pressure. This experiment should also be very helpful to identify the magnetic structures which appear at low temperatures in the TP and in the NTP phases at low and high pressures. The suppression of the Mn magnetic moment by pressure results in a drastic reduction of the molecular field at the Tb sites and opens up the possibility for the rare earth sublattice to set up different magnetic ground states depending on x.

4. Magnetic phase diagram

A magnetic phase diagram of the series $Tb_x Y_{1-x} Mn_2$ has been proposed in the past [22]. Such a magnetic phase diagram is not supported by our experimental results. We propose a new phase diagram according to our measurements. Due to the complex observed magnetic behaviour and the postulated existence of two different phases (NTP and TP) under zero pressure we show the magnetic phase diagram for each phase in figure 7(a) and 7(b) respectively. The LTE measurements provide us with the Néel temperature for the whole series. T_N does not change very much in compounds across the concentration range $0.2 \leqslant x \leqslant 1$ (≈ 45 K) but it must increase in compounds with $x \leqslant 0.2$ to reach the value of ≈ 100 K in the $x = 0$ compound. Above T_N the sample remains paramagnetic and short-range correlations seem to be suggested from LTE and MS measurements. Below T_N the magnetic structure of the TP phase depends on the yttrium content. In compounds with $x \leqslant 0.2$ it must be YMn_2-like, basically. The LTE measurements indicate that the jump at T_N is 2.5% of the sample volume in the $x = 0.2$ sample, being greater than the jump observed at concentrations beyond $x = 0.4$ ($\approx 1.5\%$) and closer to the jump in the $x = 0$ compound ($\approx 5\%$). The MS measurements show a negligible magnetostriction in compounds with $x \leqslant 0.2$ which is a distinctive feature of the YMn_2 magnetic structure. In figure 7(a) we call the YMn_2-like magnetic structure AF1. In YMn_2 the whole sample becomes transformed into AF1 [14]. In the concentration range $0.6 \leqslant x \leqslant 1$ the antiferromagnetic structure must be very close to the $TbMn_2$-like structure (we designate it AF2 in figure 7(a) and it should correspond with the previously observed S_1-like structure in $TbMn_2$ [12]). The MS measurements on the $x = 0.8$ and $x = 0.6$ compounds showed that their magnetic structure was unstable under applied field as happens in $TbMn_2$. In $TbMn_2$ part of the sample remains as NTP phase. The transition temperature T_c within the NTP phase is equal to T_N (see figure 7(b)) as it can be seen through the χ_{AC} measurements. In compounds with $x < 1$ it is to be expected to have a lower T_c for the NTP phase because the terbium content is smaller. In the $x = 0.8$ and $x = 0.6$ compounds, T_c is not directly obtained from χ_{AC} measurements at $p = 0$ kbar because at that temperature most of the sample is transformed into the TP phase and the expected peak at T_c remains too small to be observed. In the phase diagram (figure 7(b)) T_c at zero pressure for the $x = 0.8$ and $x = 0.6$ compounds is obtained from the extrapolation from the high-pressure measurements (figure 6). We also include in figure 7(b). the values of T_c measured by χ_{AC} at 7 kbar for the sake of comparison. According to the MS measurements on the $x = 0.4$ compound, the magnetic structure below T_N cannot be either AF1-like or AF2-like structure as we have already discussed in 3.2. Then we propose in figure 7(a) the existence of short-range order. Another open question is what kind of magnetic order occurs in the NTP phase of the compounds with $x < 0.6$. The loss of long-range magnetic order is to be expected with high yttrium concentrations within this phase where there is no magnetic moment at the Mn sites and the Tb governs the magnetism. This kind of behaviour has been observed in $R_x Y_{1-x} Al_2$ [29]. In figure 7(b) we propose that for $x < 0.6$ short-range magnetic order appears. This assumption needs further confirmation.

5. Conclusions

The magnetism of $Tb_x Y_{1-x} Mn_2$ compounds has been studied by means of three experimental techniques. Linear thermal expansion has allowed us to determine the temperature T_N at which the Mn atoms acquire a local magnetic moment. Surprisingly this temperature remains almost constant (≈ 40 K) for $x \geqslant 0.2$. Huge volume anomalies are observed
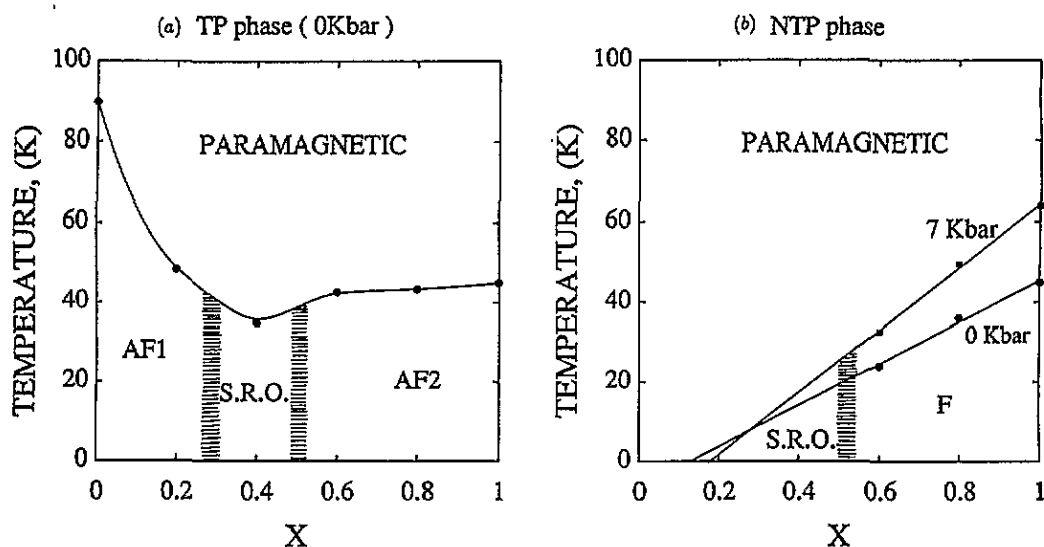
Figure 7. The magnetic phase diagram of $Tb_xY_{1-x}Mn_2$. (a) TP phase (0 kbar); (b) NTP phase (0 kbar and 7 kbar) (see text).

at T_N. Magnetostriction up to 14 T has allowed us to investigate the properties of the low-temperature magnetic structures. Below T_N the magnetic structure of compounds with $x \geqslant 0.6$ turned out to be unstable under applied magnetic field as it occurs in $TbMn_2$. As $x = 0$ (YMn_2) is approached the magnetic structure gains stability. The critical field (the field to suppress the magnetic moment on Mn below T_N) diminishes as the temperature is lowered and the yttrium content increases. We also performed AC susceptibility measurements to find transitions within the part of the sample which remains non-transformed at T_N. In $TbMn_2$ T_c is $\approx$45 K. Yet these transitions are not observed in the $x = 0.8$ and 0.6 compounds without pressure ($p = 0$ kbar) but they are visible under $p > 1$ kbar. In agreement with all these results we have proposed a magnetic phase diagram under zero pressure which suggests the YMn_2-like magnetic structure below T_N for yttrium-rich compounds ($x \leqslant 0.2$) and the $TbMn_2$-like magnetic structure for terbium-rich compounds ($x \geqslant 0.6$). A new ground state at intermediate yttrium concentrations could be present.

References

[1] Shiga M 1988 *Physica* B **149** 293–305
[2] Ritter C, Kilcoyne S H and Cywinski R 1991 *J. Phys.: Condens. Matter* **3** 727
[3] Ritter C, Mondal S, Kilcoyne S H and Cywinski R 1991 *J. Phys.: Condens. Matter* **4** 1559
[4] Terao K and Shimizu M 1983 *Phys. Lett.* **95A** 111; 1984 *Phys. Lett.* **104A** 113
[5] Yamada H, Inoue J, Terao K, Kanda S and Shimizu M 1984 *J. Phys. F: Met. Phys.* **14** 1943
[6] Yamada H 1988 *Physica* B **149** 390
[7] Chaboy J, Marcelli A, Ibarra M R and del Moral A 1994 *Solid State Commun.* **91** 859
[8] Ibarra M R, Marquina C, Algarabel P A, de Teresa J M, Ritter C and del Moral A 1994 *Proc. 13th Int. Workshop on Rare Earth Magnets and their Applications (Birmingham)* ed C A F Manwaring, D G R Jones, A J Williams and I R Harris p 127
[9] Ibarra M R, Marquina C, García-Orza L and del Moral A 1994 *J. Appl. Phys.* **75** 5662
[10] Ibarra M R, Marquina C, García-Orza L and del Moral A 1993 *Solid State Commun.* **87** 695
[11] Marquina C, Ibarra M R, de la Fuente C and del Moral A 1995 *J. Magn. Magn. Mater.* **140–144** 809

[12] Brown P J, Ouladdiaf B, Ballou R, Desportes J and Markosyan A S 1992 *J. Phys.: Condens. Matter* **4** 1103
[13] Ballou R, Brown P J, Deportes J, Markosyan A S and Ouladdiaf B 1992 *J. Magn. Magn. Mater* **104–107** 935
[14] Mondal S, Cywinski R, Kilcoyne S H, Rainford B D and Ritter C 1992 *Physica* B **180–181** 108
[15] Lelièvre-Berna E, Rouchy J and Ballou R 1994 *J. Magn. Magn. Mater.* **137** L6–10
[16] Ibarra M R, Arnold Z, Marquina C, García-Orza L and del Moral A 1994 *J. Appl. Phys.* **75** 7158
[17] Cywinski R, Kilcoyne S H and Scott C A 1991 *J. Phys.: Condens. Matter* **3** 6473
[18] Deportes J, Ouladdiaf B and Ziebeck K R A 1987 *J. Physique* **48** 1029; 1987 *J. Magn. Magn. Mater.* **70** 129
[19] Oomi G, Terada, Shiga M and Nakamura Y 1987 *J. Magn. Magn. Mater.* **70** 137
[20] Ritter C, Cywinski R, Kilcoyne S H, Mondal S and Rainford B D 1994 *Phys. Rev.* B **50** 9894
[21] Ballou R, Deportes J, Lemaire R, Rouault P and Soubeyroux J L 1990 *J. Magn. Magn. Mater.* **90 & 91** 559
[22] Belov K P, Dubenko I S, Markosyan A S and Snegirev V V 1989 *Phys. Metall. Metalloved.* **67** 108
[23] Baranov N V, Belov K P, Dubenko I S, Markosyan A S and Snegirov V V 1989 *Phys. Metall. Metalloved.* **67** 40
[24] Moriya T 1985 *Spin Fluctuations in Itinerant Electron Magnetism (Springer Series in Solid State Sciences 56)* (Berlin: Springer)
[25] Ballou R, Gaydukova I Yu, Markosyan A S and Ouladdiaf B 1992 *J. Magn. Magn. Mater.* **104–107** 1465
[26] Voiron J, Ballou R, Deportes J, Galera R M and Lelièvre E 1991 *J. Appl. Phys.* **69** 5678
[27] Callen E and Callen H B 1965 *Phys. Rev.* A **139** 455
[28] Hauser R, Bauer E, Gratz E, Haufler Th, Hilscger G and Wiesinger G 1994 *Phys. Rev.* B **50** 13 493
[29] del Moral A, Arnaudas J I, de la Fuente C, Ciria M and Joven E 1994 *J. Appl. Phys.* **76** 6180